RECENT THERMOHALINE TRENDS OF THE ATLANTIC WATERS INFLOWING TO THE MEDITERRANEAN SEA

Javier Soto-Navarro*[(1)], Francisco Criado-Aldeanueva[(1)], Jose Carlos Sánchez-Garrido[(1)] and Jesús García-Lafuente[(1)].

(1) Physical Oceanography Group, University of Málaga, Spain.

Corresponding author:
Javier Soto Navarro
Dpto. Física Aplicada II, Universidad de Málaga
E.T.S.I. Informática, Lab. 2.3.5
Campus de Teatinos s/n
29071 Málaga, Spain
Tel.: +34 952 13 28 49, Fax: +34 952 13 13 55
javiersoto@uma.es

Abstract

A total of 5077 Argo float profiles in the period 01/2002-05/2010 have been used to analyze salinity and temperature trends in the Atlantic waters adjacent to the Strait of Gibraltar in order to identify the source of recent changes observed in the inflow to the Mediterranean Sea. Positive salinity trends of 0.038±0.009 $years^{-1}$ and 0.013±0.003 $year^{-1}$ have been found for the Surface Atlantic Water and the Eastern North Atlantic Central Water, respectively. For temperature, no significant trend is observed in the surface layer and positive trend of 0.05±0.02 ºC/year is obtained for the thermocline waters. The Mediterranean Outflowing Water layer does not show any significant trend for the entire period, but a switch from positive to negative trends is observed in year 2006. In contrast to previous findings, these thermohaline variations are driven by intrinsic water masses changes, instead of isopycnal vertical displacements, probably related to an enhancement of the net freshwater losses in the area.

Introduction

The Mediterranean Sea is a semi-enclosed basin where the hydrologic budget, mainly dominated by the difference between evaporation (E) and precipitation (P), results in a water deficit that must be compensated by a net flow of Atlantic Water (AW) through the Strait of Gibraltar, its only connection with the global ocean (Bethoux and Gentilli, 1999; Mariotti et al., 2002). The AW suffers a transformation process along the basin due to the air-sea interaction that, together with the anti-estuarine exchange regime in the strait, generates a basin-scale thermohaline circulation in which the main features of the global overturning circulation take place, i.e., the deep and intermediate water formation (Bryden and Stommel 1982; García-Lafuente et al., 2007). This own circulation makes the Mediterranean Sea can be considered as a miniature ocean where

all the water masses involved are closely linked and connected to the atmospheric processes that triggers the deep convection. Since the whole system is very sensitive to changes it becomes an ideal key point for monitoring the impact of global warming (Bethoux et al., 1999). Furthermore, the Mediterranean Outflowing Water (MOW) that leaves the Strait and incorporates to the North Atlantic has an important role in the deep water formation at the Norwegian Sea as source of salinity that enhances the deep convection process, hence affecting the Meridional Overturning Circulation (MOC) and the global climate (Reid, 1979; van Aken and Beckaer, 1996; Sarafanov et al., 2008).

The Atlantic inflow through the Strait of Gibraltar is composed by Surface Atlantic Water (SAW) and Eastern North Atlantic Central Water (ENACW), the latter formed by isopycnal subduction of surface waters at northern latitudes (north to 43ºN) and incorporated to the Azores Current, the main water source to the strait area (Pollard and Pu, 1985; Paillet and Mercier, 1997; van Aken, 2001). A recent study (Millot, 2007) has detected from experimental data collected at the Moroccan continental shelf in the period 2003-2007, a high salinity trend (~0.05 $year^{-1}$) of the AW that highly exceeds the estimations for the 1990s period in the Atlantic area adjacent to the strait (Boyer et al., 2005; Poliakov et al., 2005). However, analyses of the same area in more recent periods show salinity anomalies closer to this trend (Hosoda et al., 2009; Roemmich et al., 2009) what implies a salinity input to the Mediterranean Sea that may influence the intermediate and deep water formation processes and, consequently, the characteristics of the MOW. Two main mechanisms may drive this salinity increase: changes in the intrinsic properties of the water masses or vertical displacement of the water column that makes saltier waters from the surface sink to deeper layers (Bindoff and McDougall, 1994). Here we show that the high salinity trends recorded in the Strait of

Gibraltar for the AW can also be found in the adjacent area of the North Atlantic and are more likely related to changes in the water masses properties.

Data and methods

The area of study, covering from 28ºN to 42ºN in latitude and from 5ºW to 24ºW in longitude, has been divided into three zones (Fig. 1a) to separate out the influence of the different North Atlantic circulation features in the inflowing waters through the Strait of Gibraltar. The northernmost one (zone 1 hereinafter) catches the main pathways of the MOW (Bower et al., 2002; Sarafanov et al., 2008) and the ENACW subducted northward. The central area (zone 2 hereinafter) covers the Azores Current and the southern zone (zone 3 hereinafter) covers the Canary Current (Pollard and Pu, 1985; Paillet and Mercier, 1997; van Aken, 2001). A total of 5997 ARGO salinity and temperature profiles are available at the Argo data selection web site (http://www.argodatamgt.org/) for the area from 2002 to May 2010. 15% of the profiles were neglected because they had less than ten values or were shallower than 500 m (the Argo floats cycle provides profiles from the surface to 2000 m approximately in the North Atlantic). All standard corrections detailed in the Argo Data User's Manual were applied. Moreover, data exceeding the mean profile more than three standard deviations were also erased. Once the selection was made a total of 5077 profiles covering the area of study were separated by zones and monthly distributed (Fig. 1b). The profiles were then vertically interpolated in 22 pressure levels (0 10 20 30 50 100 150 200 300 400 500 600 700 800 900 1000 1100 1200 1400 1500 1750 and 2000 dbar) and monthly averaged.

Considering the monthly averaged T-S diagram of Fig. 1c, three main water masses can be properly analyzed: Surface Atlantic Water (SAW) in the first 100 m, ENACW occupying the main thermocline from 100 to 600 m and MOW from 600 to 1200 m.

The deepest 800 m correspond to the upper layer of the North Atlantic Deep Water (NADW), mainly composed by Labrador Sea Water (LSW) although fractions of Antarctic Intermediate Water (AAIW) can be found in the lower latitudes (Machín and Pelegrí, 2008). In any case, these water masses are not completely sampled and will not be analyzed in this work. Vertically averaged time series of salinity and temperature for these layers were constructed and least-square fitted to compute their linear trends. 95% confidence intervals of this computation were estimated with a t-student test.

For comparison purposes, two additional datasets were used: i) a total of 108 CTD profiles from the French Laboratory d'Océanographie de Villefranche Dyfamed project (www.obs-vlfr.fr/sodyf/), collected at (43.25ºN, 7.52ºE) and covering the period 2001-2009 were analyzed in a similar procedure than for the Argo data, although in this case the trend was calculated only for the surface layer (0-150, Rixen et al., 2005), which corresponds to the Atlantic Water (AW) spreading through the Mediterranean Sea; ii) MOW salinity and temperature was analyzed from the time series collected at Espartel sill, western Strait of Gibraltar (35º51.70'N, 5º58.60'W), in the frame of the INGRES projects, at a mean depth of 356 m from October 2004 to February 2010.

The nature of the water properties changes at a given depth can be associated with two main different mechanisms. On one hand, modifications in the intrinsic properties of the water mass along isopycnal surfaces occupying that depth, caused by mixing or horizontal advection. On the other hand, vertical displacements of the water column that make water masses of different densities reach deeper or shallower depths without changing their intrinsic properties; this is known as isopycnal heave. It is possible to separate out the influence of these two mechanisms applying a simple model (Bindoff and McDougall, 1994).

$$\left.\frac{d\xi}{dt}\right|_p = \left.\frac{d\xi}{dt}\right|_n - \left.\frac{dp}{dt}\right|_n \left(\frac{\partial \xi}{\partial p}\right) \quad (1)$$

The left hand side term of Eq. 1 represents the time variation at isobaric surfaces of a scalar magnitude, in our case potential temperature and salinity. The first term of the right hand side represents the time variation of the magnitude along isopycnal surfaces, due to either intrinsic changes in the water mass properties or horizontal advection. The second term of the right hand side accounts for changes at a particular pressure level produced by the vertical displacement of the isopycnal surfaces.

Results and discussion

Estimated thermohaline trends

The time series for the different zones and layers are represented in Fig. 2 and the fitting results are summarized in Table 1. Whereas no significant temperature trends are observed in the surface layer, clear positive salinity trends are estimated in the complete area, 0.038±0.009 year^{-1}, and also for zones 1 and 2, of 0.010±0.005 year^{-1} and 0.04±0.01 year^{-1} respectively. Although recent studies show an increase in the salinity and temperature anomalies of the SAW in the last decade closer to our findings (Hosoda et al., 2009, Roemmich et al., 2009), these values are higher than those obtained for the 90s (Boyer et al., 2005; Poliakov et al., 2005), where positive but smaller anomalies were found. Indeed, recent measurements in the AW reaching the Mediterranean (Millot et al., 2007) provide a salinity trend of 0.05 year^{-1} for the period 2003-2007, a value very close to our result for the complete area of study and even more to that of zone 2, which corresponds with the path of the Azores Current, the main source of AW to the Mediterranean Sea (Pollard and Pu, 1985; Paillet and Mercier, 1997; van Aken, 2001).

In the ENACW layer, positive trends are observed both for salinity (with values ranging 0.005-0.013 $year^{-1}$) and temperature, about 0.05 ºC/year (Table 1). These results are also higher than those historically observed in this layer (Boyer et al., 2005; Poliakov et al., 2005), but are in good agreement with more recent estimations (Leadbetter et al., 2007; Benitez-Barrios et al., 2008). Numerical studies also predict a high intensification of the salinity anomalies for the upper 500 m of the North Atlantic in the first half of 21^{st} century (Stott et al., 2008). For the MOW, even though the computed trends for the entire period are not significant, their values are of the same order than those estimated from time series at the monitoring station of Espartel sill, the last gateway of Mediterranean waters towards the Atlantic. A positive trend of 0.0017±0.0003 ºC/year is observed for temperature and a negative trend of -0.0022±0.0003 $year^{-1}$ for salinity in the period October 2004 – February 2010 at this location (Fig. 3a). However, it is worth to mention two different periods for this layer in the whole area and zones 1 and 2: first significant positive trends from 2002 to 2006, with common values of 0.06±0.02 $years^{-1}$ and 0.2±0.1 ºC/year for salinity and temperature respectively, and a switch to negative trends from then onwards, with values around -0.05±0.02 $year^{-1}$ for salinity and -0.2±0.04 ºC/year for temperature. The increasing trend continues that of the previous period 1992-2002 in the intermediate waters of the subpolar North Atlantic, where values of 0.0088±0.0026 $year^{-1}$ for salinity and 0.049±0.01 ºC/year for temperature at 53ºN were found and attributed to a combination of MOW salinification and a low North Atlantic Oscillation (NAO) phase (Sarafanov et al., 2007).

To further investigate the influence of these results in the evolution of the thermohaline properties of the AW along the Mediterranean basin, salinity and temperature time series from the Dyfamed station corresponding to the AW layer, (the first 150 m) are represented in Fig. 3b. Positive trend of 0.016±0.008 $year^{-1}$ is found for salinity (no

171 significant trend is found for temperature). Even though this trend is smaller than our
172 estimation for the inflowing waters, it must be taken into account that the cyclonic
173 circulation of the Mediterranean Sea makes the AW reaching the Ligurian Sea differ
174 from the AW entering the Mediterranean (Millot, 1999). However, this result is one
175 order of magnitude higher than the previous estimation for the last decade of the 20th
176 century from the MEDAR-MEDATLAS dataset (Rixen et al., 2005; Vargas-Yáñez et
177 al., 2010).

178 *Mechanisms controlling changes*

179 The decomposition results of Eq. (1), displayed in Fig. 4, reveal that the observed trends
180 are strongly related to changes along isopycnal surfaces (blue), while the vertical
181 displacements (green) have a secondary role. For the complete area and zone 2 (Fig. 4a,
182 c), that exhibit similar patterns, the influence of the former mechanism is clearer, with a
183 monotonic decrease from 0.03 year^{-1} for salinity and 0.12 ºC/year for temperature at 50
184 m to almost zero at 800 m (the shallower 50 m are not considered because Eq. (1) does
185 not apply in the strong near-surface gradients, Arbic and Owens, 2001). In a previous
186 study from CTD data collected at the 36ºN section, lower temperature trends were
187 obtained for the period 1981-2005 (Leadbetter et al. 2007). But the main contrast with
188 the present work is the mechanism responsible for the trend, which in that case was the
189 isopycnal displacement. Even taking into account the differences between the sampled
190 areas, the authors estimate a negative sign for the isopycnal changes term in the first 800
191 m, opposite to our calculations, which means an important change in the thermocline
192 water characteristics of this area in the last years.

193 For zone 1 (Fig. 4b) the isopycnal heave is more important; in the first 400 m it has
194 negative sign that, for temperature, compensates the positive intrinsic changes making

the total trend zero at 200 m. For salinity the weakening of the isopycnal changes term below 600 m makes the heave responsible for the negative sign of the trend in the MOW layer. In zone 3 (Fig. 4d) the highest trend is not found at the surface, but at about 250 m, and is again caused by changes in the neutral surfaces, with negative contribution of the isopycnal displacements in the shallower 400 m, more important for temperature. From this depth, the heaving term becomes positive while the intrinsic changes term tends to zero, this leading to a small positive trend in the deeper layer for temperature. As for zone 2, studies referred to earlier periods found lower trends in this area (Vargas-Yáñez et al., 2004; Cunningham et al., 2007; Benitez- Barrios et al., 2008) with the isopycnal displacement mechanism controlling the process, especially in the ENACW layer.

The results described above emphasize that the observed trends in the SAW and in the ENACW filling the permanent thermocline, which are the main component of the Atlantic inflow to the Mediterranean, are the result of an intrinsic warming and salinification process. The existence of a salinity minimum in the bottom of the thermocline (Fig. 1c) discards the mixing with the Mediterranean water as the source of salinity for the upper layers. The most likely hypothesis for the salinity increase is an enhancement of the freshwater evaporative losses in the surface layer that increases the salinity in both SAW and ENACW by subducction processes. For the complete area, the necessary trend in the net evaporation (E-P) to match the obtained salinity trend is about 10 cm/year, a value similar to previous estimations for the 90s, which can be a consequence of an intensification of the trade winds related to a high NAO index state (Curry et al., 2003).

Conclusions

We have found that the historically observed salinity (and, in a less extent, temperature) trends of the Atlantic inflow in the Strait of Gibraltar correspond to a similar salinification/warming in the first 600 m of the surrounding Atlantic waters. The highest salinity trends are found in the surface layer of the Azores current area (0.04 $years^{-1}$), although positive values are also found northward and southward. Lower but positive values are computed in the main thermocline (around 0.01 $years^{-1}$), which in all cases exceed previous estimations. These variations are mainly related to intrinsic changes in the water masses instead of isopycnal displacements, a result that contrasts with studies carried out in earlier periods. These changes in the water masses properties are probably linked to a recent increase in the net evaporation that may affect salinity in the surface layer and also in the main thermocline by subducction and advection processes.

Acknowledgments

This work has been carried out in the frame of the P07-RNM-02938 Junta de Andalucía Spanish-funded project. Partial support from CTM2006-02326/MAR (INGRES 2) and CTM2009-05810-E projects are also acknowledged. We also acknowledge to DYFAMED (CNRS-INSU) Observatoire Océanologique de Villefranche-sur-mer for the hydrologic data used in this work.

References

Arbic, B. K., & Owens, W. B. (2001), Climatic warming of the Atlantic intermediate waters. *J. Climate. 14*, 4091-4108.

240 Benitez-Barrios, V.M., Hernández-Guerra, A., Vélez-Belchí, P., Machín, F. & Fraile-
241 Nuez, E. (2008), Recent changes in the subsurface temperature and salinity in the
242 Canary region. *Gepphys. Res. Lett. 35,* L07603.

243 Bethoux, J.P. and Gentili B., (1999**),** Functioning of the Mediterranean Sea: Past and
244 Present Changes realed to freshwater input and climatic changes. *J. Mer. Syst. 20*, 33-
245 47.

246 Bethoux, J. P., Gentilli, B., Morin, P., Nicolas, E., Pierre, C. & Ruiz-Pino, D. (1999),
247 The Mediterranean Sea: a miniature ocean for climatic and environmental studies and a
248 key for the climatic functioning of the North Atlantic. *Prog. Oceanogr. 44*, 131-146.

249 Bindoff, N. L. & McDougall, T. J. (1994), Diagnosing climate change and ocean
250 ventilation using hydrographic data, *J. Phys. Oceanogr., 24*, 1137–1152.

251 Bower, A. S., Serra, N. & Ambar, I. (2002), Structure of the Mediterranean
252 Undercurrent and Mediterranean Water spreading around the southwestern Iberian
253 Peninsula. *J. Gepphys. Res. 107,* C103161.

254 Boyer, T.P., Levitus, S., Antonov, J.I., Locarnini, R. A. & Garcia, H.E. (2005), Linear
255 trends in salinity in the World Ocean, 1955-1998. *Geophys. Res. Lett., 32,* L01604.

256 Bryden, H.L. & Stommel, H.M. (1982), Origin of the Mediterranean outflow. *J. Mar.*
257 *Res. 40*, 55–71.

258 Criado-Aldeanueva, F., Soto-Navarro, J. & García-Lafuente, J. (2011), Seasonal and
259 interannual variability of surface heat and freshwater fluxes in the Mediterranean Sea:
260 budgets and exchange through the Strait of Gibraltar. *Int. J. Climatol.* In Press.

261 Cunningham, S. A. & Alderson, S. (2007), Trasatlantic temperature and salinity
262 changes at 24.5ºN from 1957 to 2004. *Geophys. Res. Lett. 34*, L14606.

263 Curry, R., Dickson B. and Yashayaev I. (2003), A change in the freshwater balance of
264 the Atlantic Ocean over the past four decades. *Nature*. *426*, 826-829.

265 Garcíal-Lafuente, J., Sánchez-Román, A., Díaz del Río, G., Sannino G. & Sánchez-
266 Garrido, J.C. (2007), Recent observation of seasonal variability of the Mediterranean
267 outflow in the Strait of Gibraltar. *J. Geophys. Res. 112*, C10005.

268 Hosoda, S., Suga, T., Shikima, N. & Mizuno K. (2009), Global surface layer salinity
269 change detected by Argo and its implication for hydrological cycle intensification. *J.*
270 *Oceanogr*. *65*, 579-586.

271 Leadbetter, S. J., Williams, R. G., McDonagh, E. L. & King, B. A. (2007), A twenty
272 year of reversal in the water mass trends in the subtropical North Atlantic. *Geophys.*
273 *Res. Lett. 34*, L12608.

274 Machín, F. & Pelegrí, J. L. (2008), Northward penetration of Antarctic Intermediate
275 Water off Northwest Africa. *J. Phys. Oceanogr. 39*, 512-534.

276 Mariotti, A., Zeng, N. & Lau, K.M. (2002), The Hydrological cycle in the
277 Mediterranean region and implications for the water budget of the Mediterranean Sea. *J.*
278 *Climate 15*, 1674-90.

279 Millot, C. (1999), Circulation in the Western Mediterranean Sea. *J. Mar. Syst. 20*, 423-
280 442.

281 Millot C. (2007), Interannual salinification of the Mediterranean inflow. *Geophys. Res.*
282 *Lett. 34*, L21609.

283 Paillet, J. & Mercier, H. (1997), An inverse model of the eastern North Atlantic general
284 circulation and thermocline ventilation. *Deep Sea Res. Part I. 44*, 1293-1328.

285 Poliakov, I.V., Bhatt, U.S., Simmons, H.L., Ealsh, D., Waldh, J.E. & Zhang X. (2005),
286 Multidecadal Variability of North Atlantic Temperature and Salinity during the
287 Twentieth Century. *J. Climate, 18,* 4562-4581.

288 Pollard, R. T. & Pu, S. (1985), Structure and circulation of the upper Atlantic Ocean
289 northeast of the Azores. *Prog. Oceanogr. 14,* 443-462.

290 Reid, J. L. (1979), On the contribution of the Mediterranean outflow to the Norwegian-
291 Greenland Sea. *Deep Sea Res. 26*, 1199-1223.

292 Rixen, M., Bechers, J.M., Levitus, S., Antonov, J., Boyer, T., Maillard, C., Fichaut, M.,
293 Balopoulos, M., Iona, S., Dooly, S., García, M.J., Manca, B., Giorgetti, A., Manzella,
294 G., Mikhailov, N., Pinardi, N. & Zavatereli, M. (2005), The western Mediterranean
295 deep water: A proxy for climate change. *Geophys. Res. Lett. 32,* LI2608.

296 Roemmich, D. & Gilson, J. (2009), The 2004-2008 mean and annual cycle of
297 temperature, salinity, and steric height in the global ocean from the Argo program .
298 *Prog. Oceanogr., 82,* 81-100.

299 Sarafanov, A., Falina, A., Sokov, A. & Demidov, A. (2008), Intense warming and
300 salinification of intermédiate waters of southern origin in the eastern subpolar North
301 Atlantic in the 1990s to mid-2000s., *J. Gepphys. Res., 113,* C12022.

302 Stott, P.A., Sutton, R.T. & Smith, D.M. (2008), Detection and attribution of Atlantic
303 salinity changes. *Geophys. Res. Lett. 35,* L21702.

van Aken, H. M. & Beckaer, G. (1996), Hydrography and through-flow in the north-eastern North Atlantic: the NANSEN project. *Prog. Oceanogr. 38*, 297-346.

van Aken, H. M. (2001), The Hydrography of the mid-latitude Northeast Atlantic Ocean – Part III: the subducted thermocline water mass (2001), *Deep Sea Res. Part I. 48(1)*, 237-267.

Vargas-Yáñez, M., Parrilla, G., Lavín, A., Vélez-Belchí, P. & González-Pola C. (2004), Temperature and salinity increase in the eastern North Atlantic along the 24.5ºN in the last ten years. *Geophys. Res. Lett. 31*, L06210.

Vargas-Yáñez, M., Zunino, P., Belani, A., Delpy, M., Pastre, F., Moya, F., García-Martínez, & Tel, E. (2010), How much is the western Mediterranean really warming and salting? *J. Gepphys. Res., 115*, C04001.

	Complete area		Zone 1		Zone 2		Zone 3	
	S trend ($year^{-1}$)	T trend (ºC/year)	S trend ($year^{-1}$)	T trend (ºC/year)	S trend ($year^{-1}$)	T trend (ºC/year)	S trend ($year^{-1}$)	T trend (ºC/year)
0 - 100 m	0.038 ± 0.009	n.s.	0.010 ± 0.005	n.s.	0.04 ± 0.01	n.s.	n.s.	n.s.
100 - 600 m	0.013 ± 0.003	0.05 ± 0.02	0.005 ± 0.003	0.02 ± 0.01	0.013 ± 0.004	0.06 ± 0.03	0.010 ± 0.005	n.s.
600 – 1200 m	n.s.	n.s.	n.s.	n.s.	n.s.	n.s.	n.s.	n.s.
0 – Bottom	0.014 ± 0.003	0.05 ± 0.04	n.s,	n.s.	0.015 ± 0.004	0.07 ± 0.04	0.007 ± 0.006	n.s.

Table 1.Estimated linear trends for the complete area and for the zones considered. Each row corresponds to the different water masses analyzed: SAW layer (0-100 m), ENACW layer (100-600 m), MOW layer (600-1200 m) and the entire profile. The 95% confidence intervals have been computed by a *t*-student test where *n.s.* means that the fitting is not significant.

FIGURE CAPTION

FIGURE 1.Area of study, Argo profile distribution and T-S diagram. a) Selected area of study and different subzones considered. b) Monthly distribution of the Argo profiles for the complete area (top left) and for the several zones (zone 1, top right, zone 2, bottom left, and zone 3, bottom right). c) T-S diagram of the monthly averaged profiles for the complete area. The colours represent the depth in which each T-S point is found.

FIGURE 2.Time series of the monthly averaged salinity (black) and temperature (grey). a) Complete area, b) Zone 1, c) Zone 2, d) zone 3. For each zone the layers corresponding to the main water masses considered are shown: SAW (0-100 m) in the top graph of the panel, ENACW layer (100-600 m) in the second graph of the panel, MOW layer (600-1200 m) in the third graph of the panel and the entire profile in the fourth graph of the panel.

FIGURE 3.Time series of salinity and temperature from the permanent estation of Espartel sill (a) and from the Dyfamed station (b).

FIGURE 4.Results of the Eq. (1) model decomposition for salinity and temperature. a) Complete area, b) zone 1, c) zone 2 and b) zone 3. On each panel the red line represents the trend along isobaric surfaces, the blue line the contribution of changes along isopycnal surfaces and the green line the contribution of the vertical displacements. The black line is the sum of these two former contributions. The left graph of each panel represents salinity trends and the right graph temperature trends.

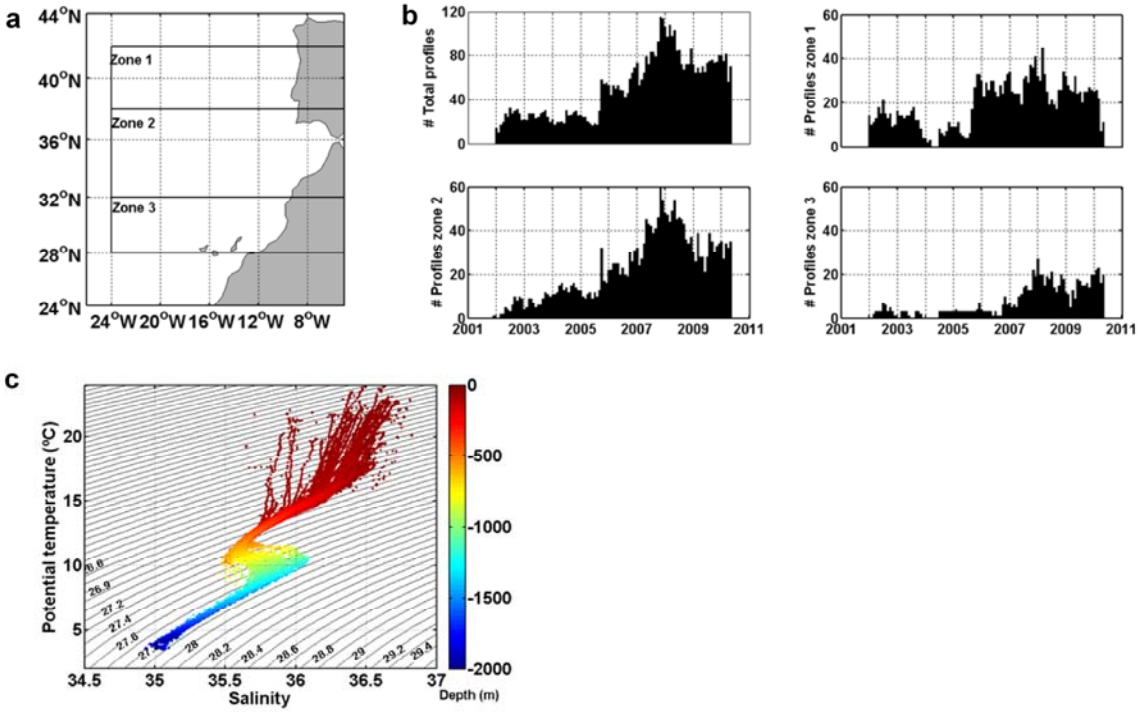
a
44°N
40°N
36°N
32°N
28°N
24°N
24°W 20°W 16°W 12°W 8°W
Zone 1
Zone 2
Zone 3
b
Total profiles
Profiles zone 1
Profiles zone 2
Profiles zone 3
2001 2003 2005 2007 2009 2011
c
Potential temperature (°C)
Salinity
Depth (m)
0
-500
-1000
-1500
-2000

Figure 1

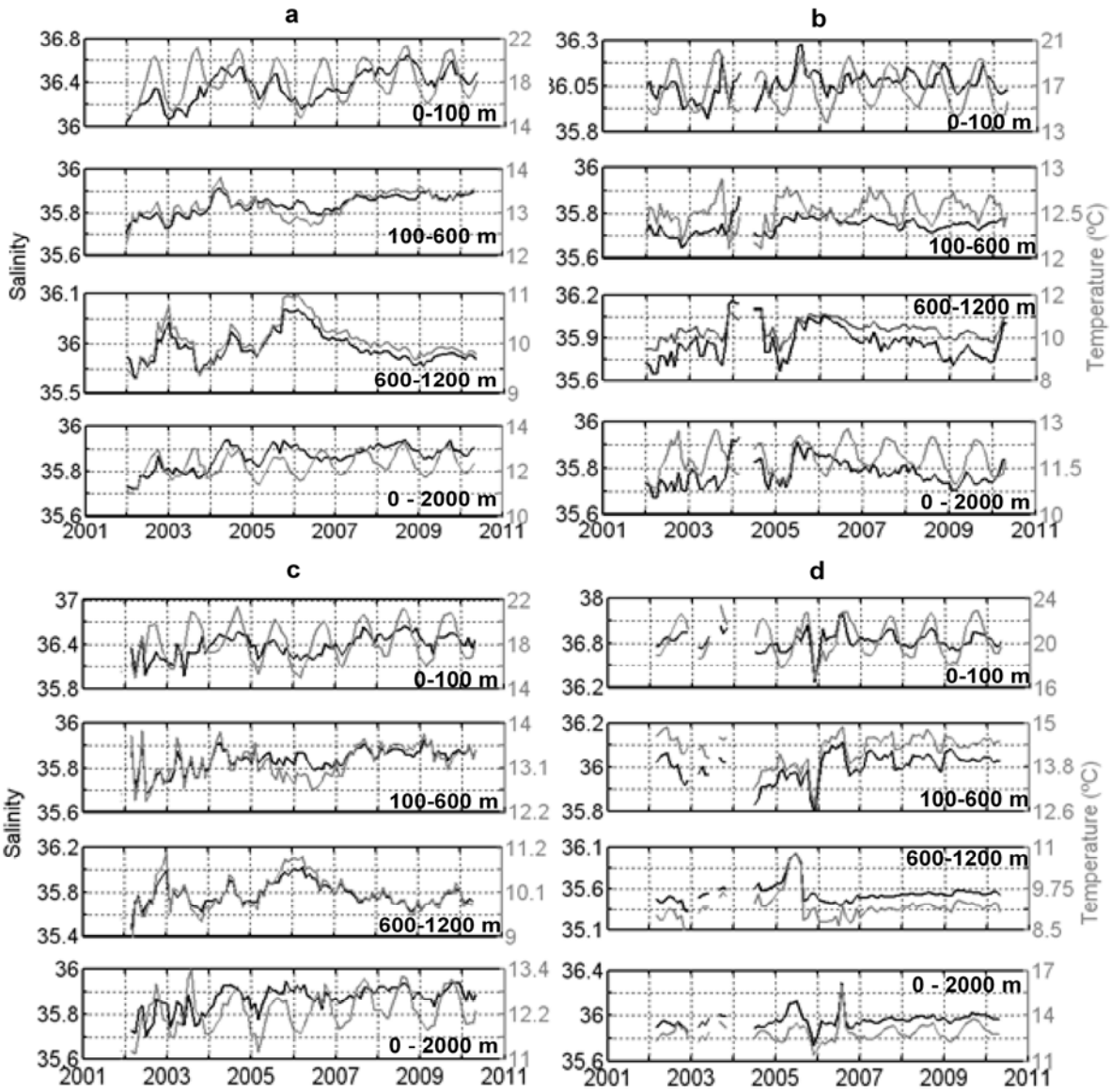
a
b
c
d
0-100 m
100-600 m
600-1200 m
0 - 2000 m
Salinity
Temperature (ºC)
2001
2003
2005
2007
2009
2011

Figure 2

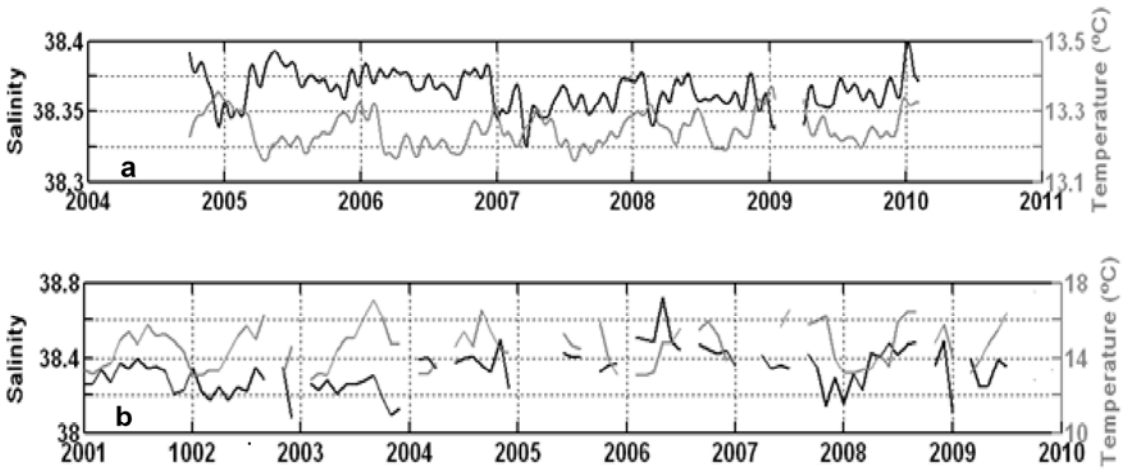

Figure 3

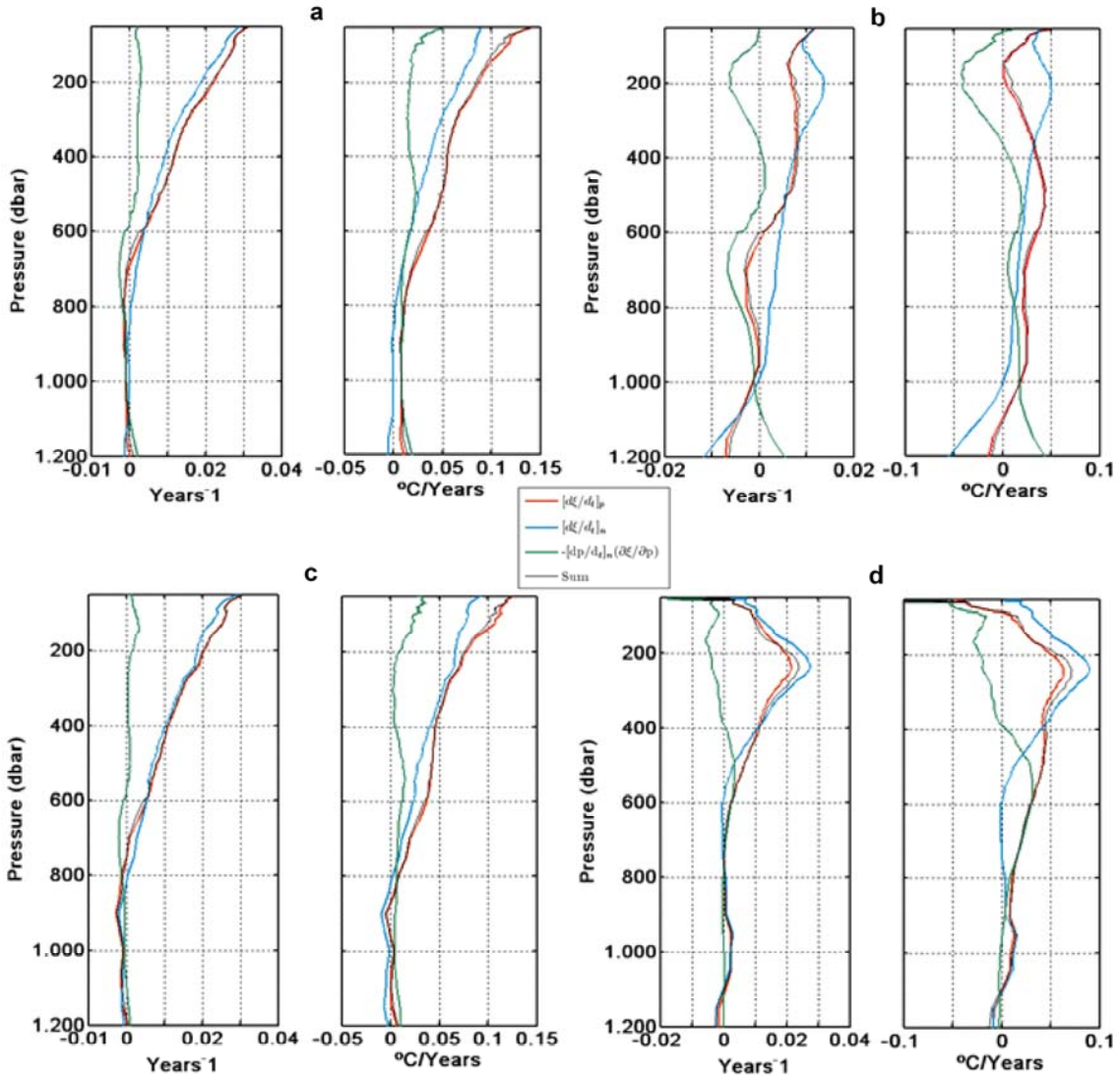

Figure 4